

UC Davis

UC Davis Previously Published Works

Title

Development of amide-based fluorescent probes for selective measurement of carboxylesterase 1 activity in tissue extracts

Permalink

<https://escholarship.org/uc/item/1v43d3p1>

Authors

Kodani, Sean D
Barthélemy, Morgane
Kamita, Shizuo G
et al.

Publication Date

2017-12-01

DOI

10.1016/j.ab.2017.10.014

Peer reviewed



HHS Public Access

Author manuscript

Anal Biochem. Author manuscript; available in PMC 2018 December 15.

Published in final edited form as:

Anal Biochem. 2017 December 15; 539: 81–89. doi:10.1016/j.ab.2017.10.014.

Development of Amide-Based Fluorescent Probes for Selective Measurement of Carboxylesterase 1 Activity in Tissue Extracts

Sean D. Kodani, Morgane Barthélemy, Shizuo G. Kamita, Bruce Hammock, and Christophe Morisseau

Department of Entomology and Nematology, and UC Davis Comprehensive Cancer Center, University of California, Davis, Davis, CA 95616, USA

Abstract

Carboxylesterases are well known for their role in the metabolism of xenobiotics. However, recent studies have also implicated carboxylesterases in regulating a number of physiological processes including metabolic homeostasis and macrophage development, underlying the need to quantify them individually. Unfortunately, current methods for selectively measuring the catalytic activity of individual carboxylesterases are not sufficiently sensitive to support many biological studies. In order to develop a more sensitive and selective method to measure the activity of human carboxylesterase 1 (hCE1), we generated and tested novel substrates with a fluorescent aminopyridine leaving group. hCE1 showed at least a 10-fold higher preference for the optimized substrate 4-MOMMP than the 13 other esterases tested. Because of the high stability of 4-MOMMP and its hydrolysis product, this substrate can be used to measure esterase activity over extended incubation periods yielding a low picogram (femtogram) limit of detection. This sensitivity is comparable to current ELISA methods; however, the new assay quantifies only the catalytically active enzyme facilitating direct correlation to biological processes. The method described herein may allow hCE1 activity to be used as a biomarker for predicting drug pharmacokinetics, early detection of hepatocellular carcinoma, and other disease states where the activity of hCE1 is altered.

Keywords

Carboxylesterase 1; Carboxylesterase 2; Fluorescent Substrate; Aminopyridines

1. Introduction

Carboxylesterases (EC 3.1.1.1) are a family of α/β -fold serine hydrolases that hydrolyze esters, amides, and thioesters [1, 2]. They generally have broad substrate selectivity and high catalytic turnover. In humans, carboxylesterase 1 (hCE1) and carboxylesterase 2 (hCE2), also

Corresponding Author: Christophe Morisseau, Ph.D., Department of Entomology, One Shields Avenue, University of California, Davis, Davis, CA 95616, FAX: 1 530 752 1537, chmorisseau@ucdavis.edu.

Publisher's Disclaimer: This is a PDF file of an unedited manuscript that has been accepted for publication. As a service to our customers we are providing this early version of the manuscript. The manuscript will undergo copyediting, typesetting, and review of the resulting proof before it is published in its final citable form. Please note that during the production process errors may be discovered which could affect the content, and all legal disclaimers that apply to the journal pertain.

termed human intestinal carboxylesterase) are the most abundantly expressed and the best studied in comparison to other carboxylesterases such as carboxylesterase 3 (hCE3), 4A, and 5 that show significantly lower expression and activity on the substrates tested [3].

Research on mammalian carboxylesterases has primarily focused on their role in xenobiotic metabolism [4]. They metabolize and increase the clearance of drugs such as methylphenidate [5] and pesticides including pyrethroids [6]. The hydrolytic activity of carboxylesterases has been utilized in the design of pro-drugs such as oseltamivir to improve bioavailability [7]. In addition to its role in xenobiotic metabolism, recent investigations of hCE1 have focused on the endogenous functions for hCE1 and its role in disease [8]. Reports have shown that glucose and lipid homeostases are regulated by *ces1* in mice, possibly implicating a role for carboxylesterases in metabolic diseases [9, 10]. Additionally, hCE1 is associated with cholesterol ester metabolism, an activity that prevents the conversion of macrophages into foam cells, which are major players in the development of atherosclerosis [11]. hCE1 has also been implicated in the progression of pulmonary arterial hypertension in methamphetamine users [12]. Finally, hCE1 is suspected to mediate tumoricidal activity in monocytes because patients with non-Hodgkins lymphoma and gastrointestinal carcinoma have altered esterase activity in these cells [13].

Thus, measuring carboxylesterase levels is not only important for predicting drug pharmacokinetics but also to foresee potential health risks and possibly to develop new disease therapies. Expression levels and activity of hCEs are affected by genetic factors and environmental factors. For example, two nonsynonymous single nucleotide polymorphisms, G143E and a frameshift mutation at Asp260, result in variants of hCE1 that show dramatic reductions in catalytic activity resulting in clinically observed increases in methylphenidate plasma levels outside of the therapeutic window [5]. Ethanol abuse has also been shown to cause changes in hCE1 activity that result in changes in drug pharmacokinetics [14]. Organophosphate and carbamate insecticides inhibit hCEs, often with higher potency than against the acetylcholinesterase (AChE) [15]. In order to identify individuals with enhanced susceptibility to the deleterious effects of hCE1-metabolized drugs and to advance studies investigating the endogenous function of hCE1, it is necessary to develop tools for selective and sensitive detection of hCE1 activity.

Several methods for the *in vitro* detection of carboxylesterases are available; however, most of these methods are not selective for the detection of hCE1 over hCE2. *p*-Nitrophenyl acetate is the most routinely used substrate that colorimetrically detects both hCE1 and hCE2 activities as well as numerous other esterases [16, 17]. More recently, substrates have been developed that employ β -elimination of cyanide, *p*-hydroxybenzyl alcohol or other function groups [18, 19]. These newer substrates, however, also show poor selectivity between hCE1 and hCE2. Other fluorescent substrates have been reported with high selectivity (approximately 10-fold) for hCE1 [20] or hCE2 [21]. Unfortunately, these substrates show low sensitivity due to high background from chemical hydrolysis. Based on a previous report [22] that hCE1 hydrolyzes lidocaine and prilocaine, both aryl amides, with much better efficiency than hCE2, we investigate here the use of aryl amides for the development of hCE1 substrates with improved selectivity without sacrificing sensitivity. Acyl aminopyridines, previously used to develop fluorescent substrates for fatty acid amide

hydrolase (FAAH) [23], were chosen due to their low background hydrolysis and intense fluorescence. The resulting substrates were compared against cyanohydrin esters that have exceptionally high activity and low background hydrolysis compared to phenyl esters [18, 24].

2. Methods

2. 1. Chemicals

2-bromo-5-nitro-6-methylpyridine, 2-bromo-5-amino-6-methylpyridine, 2-methoxy-5-amino-6-methylpyridine, 2-methoxy-5-aminopyridine, and 2-methyl-5-amino-6-methoxypyridine were purchased from AK Scientific (Union City, CA, USA). All other chemicals and reagents were synthesized in house or purchased from Acros Organics, Sigma-Aldrich or Tokyo Chemical Industry (TCI). Pooled human tissue S9 fractions were purchased from Xenotech, LLC (Lenexa, KS, USA).

2. 2. Synthetic Procedures

Corresponding fluorescent amines and cyanohydrins for **1c**, **1d**, and **1f** were prepared as previously described in Huang et al. 2009, Zanon 2003, and Shan and Hammock 2001 (Synthetic Scheme). **1b** and cyano(6-methoxynaphthalen-2-yl)methyl acetate (CMNA) were reported previously by Huang *et al.* [23] and Shan and Hammock [18]. Further experimental details, spectral characterization, and yields are provided in the Supplemental Material. All of the synthesized chemicals showed a single spot on thin layer chromatography as detected by UV absorbance on silica plates containing a green fluorescent indicator at $\lambda_{\text{abs}} = 254$ nm. In addition, H-NMR analysis did not reveal the presence of contamination.

2. 3. Preparation of Recombinant Enzymes

Recombinant baculoviruses expressing the recombinant proteins that were used in this study are previously described [23, 24]. The recombinant enzymes were produced in insect High Five cells [25] cultured in ESF921 medium (Expression Systems LLC, Davis, CA). The baculovirus-infected High Five cells were collected at 65 hours post infection by centrifugation (1000 g, 15 min, 4°C) and frozen at -80°C after decanting the medium. When needed, the cells were thawed and resuspended in 20 mM Tris-HCl buffer (pH 8.0) containing 3 mM benzamidine, 1 mM EDTA and 1 mM DDT, and homogenized using a Polytron homogenizer. The insoluble fraction after ultracentrifugation (100,000 g, 60 min, 4°C) was used as a crude preparation of FAAH. The soluble fraction was used as a crude preparation of hCE2 and hCE3. hCE1 was prepared from the insoluble pellet following ultracentrifugation (100,000 g, 60 min, 4°C) by re-suspending the pellet in 1% CHAPS (by mixing on a rotating wheel for 1 hour at 4°C). The CHAPS-soluble fraction was collected following a second ultracentrifugation (100,000 g, 60 min, 4°C) and dialyzed for 2 days in 20 mM Tris-HCl buffer (pH 8.0). The resulting solution was loaded on a DEAE anion-exchange column, and washed with 20 mM Tris-HCl buffer (pH 8.0) containing 75 mM NaCl. hCE1 was eluted with 20 mM Tris-HCl buffer (pH 8.0) containing 100 mM NaCl. Based on Coomassie brilliant blue staining of SDS-PAGE separated proteins, the purity of hCE1, hCE2, hCE3, and FAAH were estimated to be 25%, 4%, 3.5% and 6.9% respectively (Supplemental Figure 1). Other proteins (AADAC, MAGL, PON1-3) were prepared as

crude homogenized cell lysates in phosphate buffered saline (pH 7.4) and frozen at -80°C until use.

2. 4. Fluorophore Characterization

Excitation and emission maxima were determined by scanning fluorescent intensity at wavelength intervals of 2 nm using a Spectramax M2 spectrophotometer (Molecular Devices, Sunnyvale, CA) measured in 96-well medium binding, black, chimney well, flat bottom plates (Greiner Bio-One, Kremsmünster, Austria). Substrate and product stability was determined by measuring fluorescence or absorbance at 30 minute intervals for 24 hours in sodium phosphate buffer (100 mM, pH 8.0, 0.1 mg/mL BSA). The fluorescence of 6-methoxynaphthaldehyde was measured at $\lambda_{\text{exc}} = 330$ nm, $\lambda_{\text{emm}} = 465$ nm and 2-methoxy-5-amino-6-methylpyridine was measured at $\lambda_{\text{exc}} = 303$ nm, $\lambda_{\text{emm}} = 394$ nm. The absorbance of 4-nitrophenol was measured at $\lambda_{\text{abs}} = 412$ nm. Fluorescence intensities were determined using standard curves of 6-methoxynaphthaldehyde and 2-methoxy-5-amino-6-methylpyridine and absorbance intensity was determined using a standard curve of 4-nitrophenol diluted in sodium phosphate buffer (100 mM, pH 8.0, 0.1 mg/mL BSA).

2. 5. Determination of Specific Activity

Specific activity was determined by pre-diluting 5 mM substrate stock solutions in DMSO with sodium phosphate buffer (100 mM, pH 8.0, 0.1 mg/mL BSA) at a 1:14 ratio. The substrate stock solution was further diluted into wells containing enzyme in sodium phosphate buffer (100 mM, pH 8.0, 0.1 mg/mL BSA) to give $[S]_{\text{final}} = 50$ μM . Generation of fluorescence was monitored continuously at 30 second intervals for at least 10 minutes at 37°C . The values presented in the tables were calculated by correcting for the estimated purity of each recombinant enzyme (25%, 4%, 3.5%, and 6.9% purity for hCE1, hCE2, hCE3, and FAAH, respectively). All of the values shown as the average \pm standard deviation are from 3 independent experiments (each performed in triplicate) whereas values shown as a single average are from a single experiment performed in triplicate. For the experiments to determine substrate selectivity, the enzyme solutions were prepared as either a 0.1 mg/mL solution (20 μg total protein) from a commercial source or crude lysate from baculovirus-infected cells at a concentration within the linear range of the assay (300 μg). Values presented in Figure 2 and Supplemental Table 1 for AADAC, MAGL, and PON1–3 were calculated by correcting for an overall purity of 1%. This assumed purity is based on the recombinant protein expression efficiency of previous baculovirus expression experiments [24, 26]. Values were subtracted from wells containing only assay buffer and substrate. Additionally, the activity of insect cell crude lysate not infected with a baculovirus (20 μg) is presented to account for non-vector specific activity. For experiments comparing sensitivity between CMNA and 4-MOMMP, the signal-to-noise ratio was determined by taking the ratio of the mean signal in wells containing diluted enzyme to the standard deviation of the signal in wells containing enzyme but no substrate, each performed as quadruplicates of a single experiment. These limits were quantified using partially purified enzyme in the absence of any matrix.

2. 6. Western Blotting

Protein samples were prepared by dilution with 4× LDS Sample Buffer (Life Technologies, Carlsbad, CA) and 10× Reducing Buffer (Life Technologies, Carlsbad, CA) and were subsequently boiled. Samples were run at 200 V for 35 minutes on Bolt 4–12% Bis-Tris Gels (Life Technologies, Carlsbad, CA) in MOPS running buffer, and transferred to nitrocellulose membranes. The membranes were then blocked with 3% BSA, incubated with rabbit polyclonal anti-human CES1 antibody (1:5000) and subsequently incubated with secondary goat anti-rabbit IgG (1:5000) (Abcam, Cambridge, MA). Anti-human CES1 antibody was prepared in a manner previously described [12, 27]. Membranes were imaged on a ChemiDoc MP (Bio-Rad, Hercules, CA) using SuperSignal West Femto ECL Detection Reagent (Thermo Scientific, Waltham, MA). Quantification of band intensity was performed using ImageLab 5.0 (Bio-Rad, Hercules, CA). Values are given as average ± standard deviation, and represent at least 2 independent gels.

2. 7. Measuring Potency of Esterase Inhibitors

Median inhibitor concentration (IC_{50}) values were determined by the addition of enzyme to serially diluted solutions (2-fold) of inhibitor with the maximum inhibitor concentration either at 100 μ M or 4-times the IC_{50} , whichever was lower. Enzyme-inhibitor solutions were incubated for 5 minutes before the addition of CMNA for hCE1, hCE2, hCE3, AADAC and PON1 ($[S]_{final} = 50 \mu$ M in 2 μ L DMSO, $[DMSO]_{final} = 2\%$) or **1b** for FAAH ($[S]_{final} = 50 \mu$ M in 2 μ L DMSO, $[DMSO]_{final} = 2\%$). Substrate formation was measured kinetically over 10 minutes (CMNA, $\lambda_{exc} = 330$ nm, $\lambda_{emm} = 465$ nm; **1b**, $\lambda_{exc} = 303$ nm, $\lambda_{emm} = 394$ nm). Final IC_{50} values were calculated by simple linear regression of log [Inhibitor] against % remaining activity. The values represent the average of triplicates from a single experiment.

3. Results

3. 1. Optical Properties of Fluorophores

Substituted amino-pyridines, including **I** and **II**, have been previously used for enzyme assays due to their intense fluorescence, high Stokes shift and the substantial difference between fluorescence as free amines and amides [23, 28]. Additionally, their excitation and emission wavelength maxima are above the intrinsic absorbance of most cellular components, reducing the background interference of cell extracts. To modify the fluorescence intensity of **I**, the 6-methoxy group was replaced with either an electron withdrawing group (cyano, **III**) or electron donating group (dimethylamino, **IV**). Neither modification resulted in an increase in fluorescent intensity (Table 1); however, **III** had marginally lower excitation/emission wavelengths while **IV** had marginally higher excitation/emission wavelengths. Additionally, the aminopyridine with methoxy and methyl substitutions in the 2- and 6-positions, respectively, (**V**) was 4-fold less fluorescent.

3. 2. Effect of Fluorophore on Enzyme Activity and Selectivity

To investigate the effect of different substituents on the pyridine fluorophore on enzyme activity and selectivity, the turnover of octyl-amide substrates was measured for hCE1, hCE2, and hCE3 (Table 2). Additionally, since **1b**, the methoxypyridinyl amide without the

2-methyl substitution, is a reported substrate for the endocannabinoid-metabolizing enzyme fatty acid amide hydrolase (FAAH) [23], activities were also compared to FAAH. While **1b** was 20-fold more selective for FAAH than for hCE1, addition of the methyl group in the 2-position (**1a**) resulted in 10-fold higher selectivity of hCE1 over FAAH. Switching the 2-methyl and 6-methoxy groups (**1e**) resulted in 3-fold higher specific activity for hCE1; however, the fluorescence intensity of **V** is 4-fold less than that of **I**, resulting in slightly lower overall signal intensity. Additionally, exchanging the 6-methoxy group with the strongly activating dimethylamino (**1d**) and strongly deactivating cyano (**1c**) resulted in substantially reduced activity. Since cyanohydrin esters have been used for characterizing carboxylesterase [24], activities were measured for the corresponding octanoate ester (**1f**). Although the ester substrate had the highest turnover by hCE2, its turnover by hCE1 was comparable to that of the best amide substrates (**1e**).

3. 3. Effect of Acyl Chain on Substrate Selectivity

To increase selectivity for hCE1 over the other enzymes, amides of varying size were synthesized and their turnover rates compared between hCE1, hCE2, and hCE3 (Table 3). The acyl chains consisted of various straight chains (**2–9**), with terminal phenyl groups (**12–18**), and complex chains (**10, 11, 19, 20**). Generally, hCE1 preferred medium chain amides (7–10 carbons), hCE2 had relatively equivalent activity for acyl chains that were 6–14 carbons long, and hCE3 preferred long chain amides (9+ carbons). Bulky short chain amides were poor substrates for all three enzymes (**10–11**). Increasing steric bulk by either adding a benzene ring to the terminal position of the chain or adding a secondary carbon in the middle of the 8-carbon chain increased enzyme selectivity towards hCE1 over hCE2 and hCE3 (**12–18, 19**); however, it did not increase overall enzymatic turnover. Adding a thioether functional group on the β -position of the carbon chain has been previously shown to improve the potency on inhibitors of esterases [29]. To determine whether the same functional group also improves the turnover of substrates, we modified the octanamide to the corresponding β -thioether (**20**). This modification increased the specific activity on hCE1 by 13%, but reduced overall selectivity. By comparing the kinetic parameters, K_M and V_{max} , between **1a, 19**, and **20** and the general esterase substrate CMNA, we found the selectivity between the carboxylesterases was primarily due to differences in V_{max} (Table 4). Interestingly, replacement of an ester by an amide resulted in an over 1,000-fold loss of activity for hCE2 but only a 5–20 fold loss for hCE1. For further experiments, 4-MOMMP (**19**) was investigated due to its high activity and high selectivity.

3. 4. Sensitivity and Kinetics of 4-MOMMP (19) Hydrolysis

The catalytic efficiency of hCE1 acting on 4-MOMMP is approximately 16-fold lower than that of CMNA. After accounting for difference in fluorescence intensity, there is an overall 4-fold higher limit of quantification using 4-MOMMP (Table 5) for hCE1 when measuring in kinetic mode for a short time (<30 minutes). This is mostly due to a 3-fold lower V_{max} for **19** (Table 4). However, 4-MOMMP has a low background hydrolysis (200-fold lower than CMNA) (Figure 1B), and its fluorescent product **V** has a high stability in buffer (Figure 1A), especially compared to the fluorescent product from CMNA, 6-methoxynaphthaldehyde. The decomposition of 6-methoxynaphthaldehyde signal over long periods of time is due to

the presence of protein in the assay solution [30]. Thus, background noise of 4-MOMMP is substantially reduced and the dynamic range remained high even over a long period of time (100-fold, $R^2 > 0.99$). Consequently, while hCE1 hydrolysis of 4-MOMMP remained linear for at least 24 hours, the hydrolysis of CMNA was substantially diminished after 4 hours (Supplemental Figure 3). Phenolic esters such as 4-nitrophenyl acetate (4-NPA) are commonly used as general substrates for esterases. They have high product stability but their limit of detection is limited due to high background hydrolysis compared to CMNA (Figure 1). Although the amide substrates have generally lower activity than ester substrates, their high chemical stability, thus low background hydrolysis, makes them an attractive option for assays with higher sensitivity requiring long incubation periods. Consequently, increasing the reaction time to 24 hours and measuring activity as an endpoint assay, rather than in kinetic mode, dramatically increased the overall signal and increased the limit of detection of hCE1 by 4-MOMMP to low picogram levels (Table 5).

3. 5. Selectivity of 4-MOMMP (19) for hCE1

To evaluate the overall selectivity of 4-MOMMP for hCE1, activity was measured with crude and commercially obtained preparations of carboxylesterases and various serine hydrolases (Figure 2, Supplemental Table 1). 4-MOMMP showed substantially higher selectivity for hCE1 compared to all of the other esterases tested (Figure 2A). FAAH had the second highest activity, with 10-fold lower turnover than hCE1. In comparison, the CMNA substrate previously developed in this laboratory [18] showed poor selectivity for hCE1, hCE2, AADAC, and PON2 (Figure 2B). Similarly, 4-NPA showed high specific activity for hCE1, hCE2, AADAC, PON2, and PON3 (Figure 2C), thus, poor selectivity. In order to validate the usefulness of 4-MOMMP to selectively quantify hCE1, the activities of commercial pooled S-9 samples of liver, intestine, kidney and lung were determined (Table 6). After correcting for % purity as determined by band densitometry of Coomassie brilliant blue stained gels (Supplementary Figure 1), the specific activities for hCE1 and hCE2 were within 2-fold of those previously reported (Table 6) [24]. By western blot analysis, hCE1 expression was highest in liver followed by lung, intestine, and kidney. Correspondingly, hydrolysis of 4-MOMMP was highest in the liver, detectable in the lung, and undetectable in the intestine and kidney. In comparison, when CMNA was used as a substrate, hydrolysis by hCE1 appeared to be overestimated in the lung, kidney, and intestine by 5-, 25-, and 60-fold, respectively. Cross-reactivity of the hCE1 antibody with hCE2 and hCE3 was low (Supplementary Figure 2) and thus hCE2 and hCE3 proteins contributed relatively little to the Western blot estimation.

3. 6. Use of Inhibitors to Improve Selectivity

An alternative approach to selectively quantify hCE1 is to use inhibitors to remove contaminating activity (i.e., non-hCE1 esterase activity). Toward this goal, we measured the potency of several previously described inhibitors against hCE1, hCE2, AADAC, and several esterases against which the chemicals were previously untested (Table 7). The relative potency of 2-chloro-3',4'-dimethoxybenzil, loperamide, and thyroxine for hCE2 relative to hCE1 were similar to values previously found in the literature [31, 32]. Combining **19** and loperamide, the contaminating activity with 100-fold excess hCE2 is only 30% of the original compared to 90% without loperamide (Figure 3). It is worth noting that

although 2-chloro-3',4'-dimethoxybenzil and loperamide selectively inhibited hCE2 over hCE1, these inhibitors showed relatively low potency on other carboxylesterases. Thus, this approach is effective at eliminating contaminating activity against hCE2 but does not eliminate activity for other esterases.

4. Discussion

Here, we identified 4-MOMMP (**19**) as a novel substrate for hCE1 that can be used to quantify selectively hCE1 activity in tissues. Although the turnover of 4-MOMMP by hCE1 is 10 times lower than the model general esterase substrate CMNA, its strong chemical stability allows to quantify low picogram levels of hCE1 when using an endpoint measurement over 24 hours. Additionally, its turnover by hCE1 is at least 10-fold more selective compared to the 13 different serine hydrolases that we tested and 40- to 50-fold more selective compared to hCE2. This selectivity was confirmed by comparing the relative amounts of hCE1 in tissues as measured by 4-MOMMP to the estimated quantity by western blot analyses and previously reported values [16]. Of the other enzymes that hydrolyzed 4-MOMMP, FAAH had the highest activity. This is expected considering the endogenous substrates for FAAH are amides similar to 4-MOMMP [33]. One approach for reducing contaminating activity is the addition of selective inhibitors for off-target enzymes to the reaction mixture. In addition to using loperamide to remove hCE2 activity, a large variety of selective inhibitors for FAAH are available [34–36]. However, these inhibitors only reduce the signal from a single target and would not be effective as a replacement for a highly selective substrate.

A number of studies have previously investigated the structural relationship of various ester and amide substrates that are hydrolyzed by hCE1 and hCE2 [37–39]. Generally, hCE1 is most active on esters containing small acid and large alcohol groups, while hCE2 best hydrolyzes esters with large acids and small alcohols [2]. For the amide substrates examined in this study, the length of the acyl chain and the size of the free amide poorly correlated with specificity for one enzyme over the other. Instead, it appeared that the relatively high reactivity of hCE1 on the aminopyridine substrates relative to hCE2 allows for specificity for these substrates. In the case of 4-MOMMP, the K_M for hCE2 was 3-fold lower than that of hCE1 and the difference in V_{max} was 120-fold higher with hCE1. Thus, V_{max} is the primary contributor to the higher selectivity. While carboxylesterases are primarily ester metabolizing enzymes, the relatively high turnover of these amide substrates demonstrates hCE1 also should be considered when characterizing metabolism of amide xenobiotics.

The ability to selectively measure hCE1 activity using 4-MOMMP could allow hCE1 to be used as a biomarker to predict the pharmacokinetics of drugs and the status of some diseases in patients. As previously mentioned, two SNPs are associated with reduced hCE1 activity that results in altered pharmacokinetics of ester containing drugs [40]. Although the frequency of these SNPs in the general population is rare, the potential adverse drug effects associated with poor metabolism may be severe. By using 4-MOMMP to screen individuals for hCE1 activity, rather than hCE1 protein levels by ELISA, clinicians could reduce the likelihood for adverse drug reactions in patients prior to receiving drug treatment. Additionally, hCE1 abundance in the plasma has been identified as a potential biomarker for

hepatocellular carcinoma [41]. The detection limit of the catalytic assay described in this study with 4-MOMMP is well within the reported detection limit (8 ng/mL) of ELISA. The 4-MOMMP assay described in this study measures catalytically active enzyme, requires fewer steps and less costly reagents, and does not require an antibody when compared to ELISA.

Supplementary Material

Refer to Web version on PubMed Central for supplementary material.

Acknowledgments

Funding: This work was supported in part by the National Institute of Environmental Health Sciences ES002710, the CounterACT Program U5 NS079202 and the National Institute of Environmental Health Sciences Superfund Research Program P42 ES004699. SDK was supported by a NIGMS-funded Pharmacology Training Program T32GM099608.

Abbreviations and definitions

AADAC	arylacetamide deacetylase
AChE	acetylcholinesterase
CMNA	cyano(6-methoxynaphthalen-2-yl)methyl acetate (Table 2)
ELISA	enzyme-linked immunosorbent assay
FAAH	fatty acid amide hydrolase
hCE1	carboxylesterase 1
hCE2	carboxylesterase 2
hCE3	carboxylesterase 3
MAGL	monoacylglycerol lipase
4-MOMMP	N-(6-methoxy-2-methylpyridin-3-yl)-4-methyloctanamide (structure 19 in Table 3)
4-NPA	4-nitrophenyl acetate
PON1	paraoxonase 1
PON2	paraoxonase 2
PON3	paraoxonase 3.

Literature Cited

1. Ross MK, Streit TM, Herring KL. Carboxylesterases: Dual roles in lipid and pesticide metabolism. *J Pestic Sci.* 2010; 35:257–264. [PubMed: 25018661]
2. Satoh T, Hosokawa M. Structure, function and regulation of carboxylesterases. *Chem Biol Interact.* 2006; 162:195–211. [PubMed: 16919614]

3. Holmes RS, Wright MW, Laulederkind SJ, Cox LA, Hosokawa M, Imai T, Ishibashi S, Lehner R, Miyazaki M, Perkins EJ, Potter PM, Redinbo MR, Robert J, Satoh T, Yamashita T, Yan B, Yokoi T, Zechner R, Maltais LJ. Recommended nomenclature for five mammalian carboxylesterase gene families: human, mouse, and rat genes and proteins. *Mamm Genome*. 2010; 21:427–441. [PubMed: 20931200]
4. Hatfield MJ, Umans RA, Hyatt JL, Edwards CC, Wierdl M, Tsurkan L, Taylor MR, Potter PM. Carboxylesterases: General detoxifying enzymes. *Chem Biol Interact*. 2016; 259:327–331. [PubMed: 26892220]
5. Zhu HJ, Patrick KS, Yuan HJ, Wang JS, Donovan JL, DeVane CL, Malcolm R, Johnson JA, Youngblood GL, Sweet DH, Langae TY, Markowitz JS. Two CES1 gene mutations lead to dysfunctional carboxylesterase 1 activity in man: clinical significance and molecular basis. *Am J Hum Genet*. 2008; 82:1241–1248. [PubMed: 18485328]
6. Ross MK, Borazjani A, Wang R, Crow JA, Xie S. Examination of the carboxylesterase phenotype in human liver. *Arch Biochem Biophys*. 2012; 522:44–56. [PubMed: 22525521]
7. Suzaki Y, Uemura N, Takada M, Ohyama T, Itohda A, Morimoto T, Imai H, Hamasaki H, Inano A, Hosokawa M, Tateishi M, Ohashi K. The effect of carboxylesterase 1 (CES1) polymorphisms on the pharmacokinetics of oseltamivir in humans. *Eur J Clin Pharmacol*. 2013; 69:21–30. [PubMed: 22673926]
8. Lian J, Nelson R, Lehner R. Carboxylesterases in lipid metabolism: from mouse to human. *Protein Cell*. 2017; doi: 10.1007/s13238-017-0437-z
9. Xu J, Li Y, Chen WD, Xu Y, Yin L, Ge X, Jadhav K, Adorini L, Zhang Y. Hepatic carboxylesterase 1 is essential for both normal and farnesoid X receptor-controlled lipid homeostasis. *Hepatology*. 2014; 59:1761–1771. [PubMed: 24038130]
10. Xu J, Yin L, Xu Y, Li Y, Zalzal M, Cheng G, Zhang Y. Hepatic carboxylesterase 1 is induced by glucose and regulates postprandial glucose levels. *PLoS One*. 2014; 9:e109663. [PubMed: 25285996]
11. Crow JA, Middleton BL, Borazjani A, Hatfield MJ, Potter PM, Ross MK. Inhibition of carboxylesterase 1 is associated with cholesteryl ester retention in human THP-1 monocyte/macrophages. *Biochim Biophys Acta*. 2008; 1781:643–654. [PubMed: 18762277]
12. Orcholski ME, Khurshudyan A, Shamskhov EA, Yuan K, Chen IY, Kodani SD, Morisseau C, Hammock BD, Hong EM, Alexandrova L, Alastalo TP, Berry G, Zamanian RT, de Jesus Perez VA. Reduced Carboxylesterase 1 Is Associated with Endothelial Injury in Methamphetamine Induced Pulmonary Arterial Hypertension. *Am J Physiol Lung Cell Mol Physiol*. 2017; 313:L252–L266. [PubMed: 28473326]
13. Markey GM. Carboxylesterase 1 (Ces1): from monocyte marker to major player. *J Clin Pathol*. 2011; 64:107–109. [PubMed: 2117752]
14. Patrick KS, Straughn AB, Minhinnett RR, Yeatts SD, Herrin AE, DeVane CL, Malcolm R, Janis GC, Markowitz JS. Influence of ethanol and gender on methylphenidate pharmacokinetics and pharmacodynamics. *Clin Pharmacol Ther*. 2007; 81:346–353. [PubMed: 17339864]
15. Cashman JR, Perotti BYT, Berkman CE, Lin J. Pharmacokinetics and Molecular Detoxication. *Environ Health Perspect*. 1996; 104:23–40. [PubMed: 8722108]
16. Watanabe A, Fukami T, Nakajima M, Takamiya M, Aoki Y, Yokoi T. Human arylacetamide deacetylase is a principal enzyme in flutamide hydrolysis. *Drug Metab Dispos*. 2009; 37:1513–1520. [PubMed: 19339378]
17. Kroetz DL, McBride OW, Gonzalez FJ. Glycosylation-Dependent Activity of Baculovirus-Expressed Human Liver Carboxylesterases: cDNA Cloning and Characterization of Two Highly Similar Enzyme Forms. *Biochemistry*. 1993; 32:11606–11617. [PubMed: 8218228]
18. Shan G, Hammock BD. Development of sensitive esterase assays based on alpha-cyano-containing esters. *Anal Biochem*. 2001; 299:54–62. [PubMed: 11726184]
19. Zhang Y, Chen W, Feng D, Shi W, Li X, Ma H. A spectroscopic off-on probe for simple and sensitive detection of carboxylesterase activity and its application to cell imaging. *Analyst*. 2012; 137:716–721. [PubMed: 22159212]

20. Liu ZM, Feng L, Ge GB, Lv X, Hou J, Cao YF, Cui JN, Yang L. A highly selective ratiometric fluorescent probe for in vitro monitoring and cellular imaging of human carboxylesterase 1. *Biosens Bioelectron.* 2014; 57:30–35. [PubMed: 24534577]
21. Feng L, Liu ZM, Hou J, Lv X, Ning J, Ge GB, Cui JN, Yang L. A highly selective fluorescent ES IPT probe for the detection of Human carboxylesterase 2 and its biological applications. *Biosens Bioelectron.* 2014; 65C:9–15.
22. Higuchi R, Fukami T, Nakajima M, Yokoi T. Prilocaine- and lidocaine-induced methemoglobinemia is caused by human carboxylesterase-, CYP2E1-, and CYP3A4-mediated metabolic activation. *Drug Metab Dispos.* 2013; 41:1220–1230. [PubMed: 23530020]
23. Huang H, Nishi K, Tsai HJ, Hammock BD. Development of highly sensitive fluorescent assays for fatty acid amide hydrolase. *Anal Biochem.* 2007; 363:12–21. [PubMed: 17291440]
24. Nishi K, Huang H, Kamita SG, Kim IH, Morisseau C, Hammock BD. Characterization of pyrethroid hydrolysis by the human liver carboxylesterases hCE-1 and hCE-2. *Arch Biochem Biophys.* 2006; 445:115–123. [PubMed: 16359636]
25. Granados RR, Guoxon L, Derksen ACG, McKenna KA. A New Insect Cell Line from *Trichoplusia ni* (BTI-Tn-5B1-4) Susceptible to *Trichoplusia ni* Single Enveloped Nuclear Polyhedrosis Virus. *J Invertebr Pathol.* 1994; 64:260–266.
26. Stok JE, Huang H, Jones PD, Wheelock CE, Morisseau C, Hammock BD. Identification, expression, and purification of a pyrethroid-hydrolyzing carboxylesterase from mouse liver microsomes. *J Biol Chem.* 2004; 279:29863–29869. [PubMed: 15123619]
27. Zhu W, Song L, Zhang H, Matoney L, LeCluyse E, Yan B. Dexamethasone Differentially Regulates Expression of Carboxylesterase Genes in Humans and Rats. *Drug Metab Dispos.* 2000; 28:186–191. [PubMed: 10640517]
28. Huang H, Tanaka H, Hammock BD, Morisseau C. Novel and highly sensitive fluorescent assay for leucine aminopeptidases. *Anal Biochem.* 2009; 391:11–16. [PubMed: 19433052]
29. Hammock BD, Wing KD, McLaughlin J, Lovell VM, Sparks TC. Trifluoromethylketones as Possible Transition State Analog Inhibitors of Juvenile Hormone Esterase. *Pest Biochem Physiol.* 1982; 17:76–88.
30. Wheelock CE, Wheelock AM, Zhang R, Stok JE, Morisseau C, Le Valley SE, Green CE, Hammock BD. Evaluation of α -cyanoesters as fluorescent substrates for examining interindividual variation in general and pyrethroid-selective esterases in human liver microsomes. *Anal Biochem.* 2003; 315:208–222. [PubMed: 12689831]
31. Wadkins RM, Hyatt JL, Edwards CC, Tsurkan L, Redinbo MR, Wheelock CE, Jones PD, Hammock BD, Potter PM. Analysis of mammalian carboxylesterase inhibition by trifluoromethylketone-containing compounds. *Mol Pharmacol.* 2007; 71:713–723. [PubMed: 17167034]
32. Shimizu M, Fukami T, Nakajima M, Yokoi T. Screening of specific inhibitors for human carboxylesterases or arylacetamide deacetylase. *Drug Metab Dispos.* 2014; 42:1103–1109. [PubMed: 24751575]
33. Piomelli D, Sasso O. Peripheral gating of pain signals by endogenous lipid mediators. *Nat Neurosci.* 2014; 17:164–174. [PubMed: 24473264]
34. Ahn K, Johnson DS, Mileni M, Beidler D, Long JZ, McKinney MK, Weerapana E, Sadagopan N, Liimatta M, Smith SE, Lazerwith S, Stiff C, Kamtekar S, Bhattacharya K, Zhang Y, Swaney S, Van Becelaere K, Stevens RC, Cravatt BF. Discovery and characterization of a highly selective FAAH inhibitor that reduces inflammatory pain. *Chem Biol.* 2009; 16:411–420. [PubMed: 19389627]
35. Johnson DS, Stiff C, Lazerwith SE, Kesten SR, Fay LK, Morris M, Beidler D, Liimatta MB, Smith SE, Dudley DT, Sadagopan N, Bhattachar SN, Kesten SJ, Nomanbhoy TK, Cravatt BF, Ahn K. Discovery of PF-04457845: A Highly Potent, Orally Bioavailable, and Selective Urea FAAH Inhibitor. *ACS Med Chem Lett.* 2011; 2:91–96. [PubMed: 21666860]
36. Keith JM, Apodaca R, Xiao W, Seierstad M, Pattabiraman K, Wu J, Webb M, Karbarz MJ, Brown S, Wilson S, Scott B, Tham CS, Luo L, Palmer J, Wennerholm M, Chaplan S, Breitenbucher JG. Thiadiazolopiperazinyl ureas as inhibitors of fatty acid amide hydrolase. *Bioorg Med Chem Lett.* 2008; 18:4838–4843. [PubMed: 18693015]

37. Imai T, Taketani M, Shii M, Hosokawa M, Chiba K. Substrate specificity of carboxylesterase isozymes and their contribution to hydrolase activity in human liver and small intestine. *Drug Metab Dispos.* 2006; 34:1734–1741. [PubMed: 16837570]
38. Huang T, Shiotsuki T, Uematsu T, Borhan B, Li QX, Hammock BD. Structure-Activity Relationships for Substrates and Inhibitors of Mammalian Liver Microsomal Carboxylesterases. *Pharm Res.* 1996; 13:1495–1500. [PubMed: 8899840]
39. Hosokawa M. Structure and Catalytic Properties of Carboxylesterase Isozymes Involved in Metabolic Activity of Prodrugs. *Molecules.* 2008; 13:412–431. [PubMed: 18305428]
40. Zhu HJ, Appel DI, Johnson JA, Chavin KD, Markowitz JS. Role of carboxylesterase 1 and impact of natural genetic variants on the hydrolysis of trandolapril. *Biochem Pharmacol.* 2009; 77:1266–1272. [PubMed: 19185566]
41. Na K, Lee EY, Lee HJ, Kim KY, Lee H, Jeong SK, Jeong AS, Cho SY, Kim SA, Song SY, Kim KS, Cho SW, Kim H, Paik YK. Human plasma carboxylesterase 1, a novel serologic biomarker candidate for hepatocellular carcinoma. *Proteomics.* 2009; 9:3989–3999. [PubMed: 19658107]

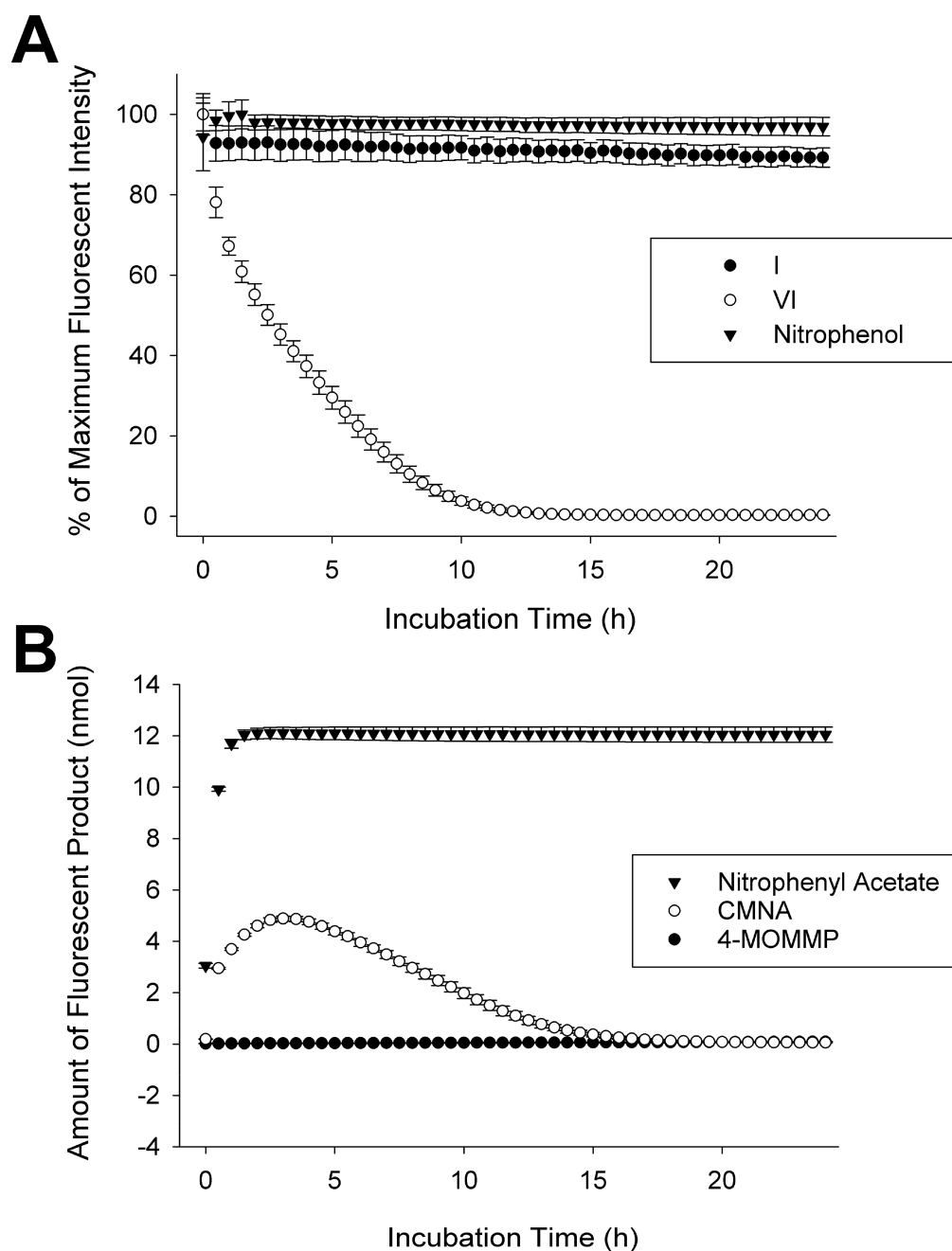


Figure 1. (A) Chemical stability of nitrophenol, VI and I in phosphate buffer (100 mM, pH = 8, 0.1 mg/mL BSA) over 24 hours. (B) Background hydrolysis of CMNA, 4-NPA and 4-MOMMP in phosphate buffer (100 mM, pH = 8, 0.1 mg/mL BSA). Rates of background hydrolysis are 610 pmol/min (4-NPA), 20 pmol/min (CMNA) and 0.1 pmol/min (4-MOMMP). Results are representative of the average of 6 replicates (\pm standard deviation) run in a single experiment.

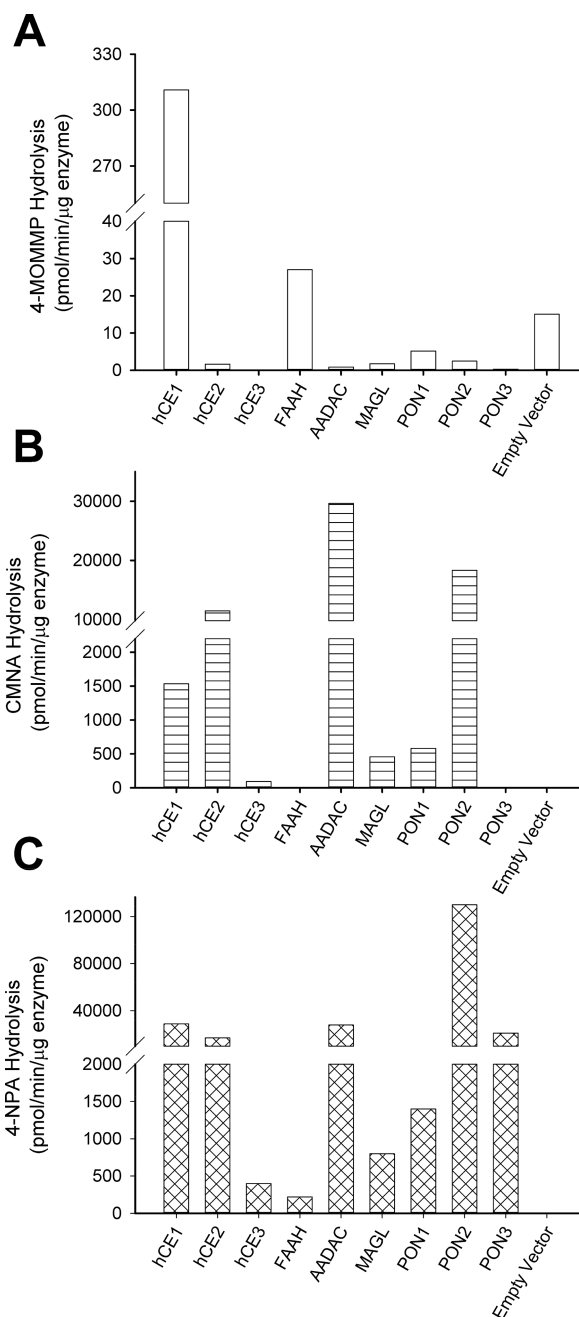


Figure 2. Rate of hydrolysis of (A) 4-MOMMP, (B) CMNA, and (C) 4-NPA for multiple esterases. Partially purified (hCE1) or crude enzyme extract (hCE2, hCE3 FAAH, AADAC, MAGL, PON1, PON2, and PON3) was added to 50 μ M of either substrate in phosphate buffer (100 mM, pH = 8, 0.1 mg/mL BSA) and the formation of product was measured over 10 minutes. The purity of each enzyme was estimated on the basis of the analyses of Coomassie brilliant blue staining of crude enzyme extracts separated by SDS-PAGE. Values represent the average of triplicates for a single experiment.

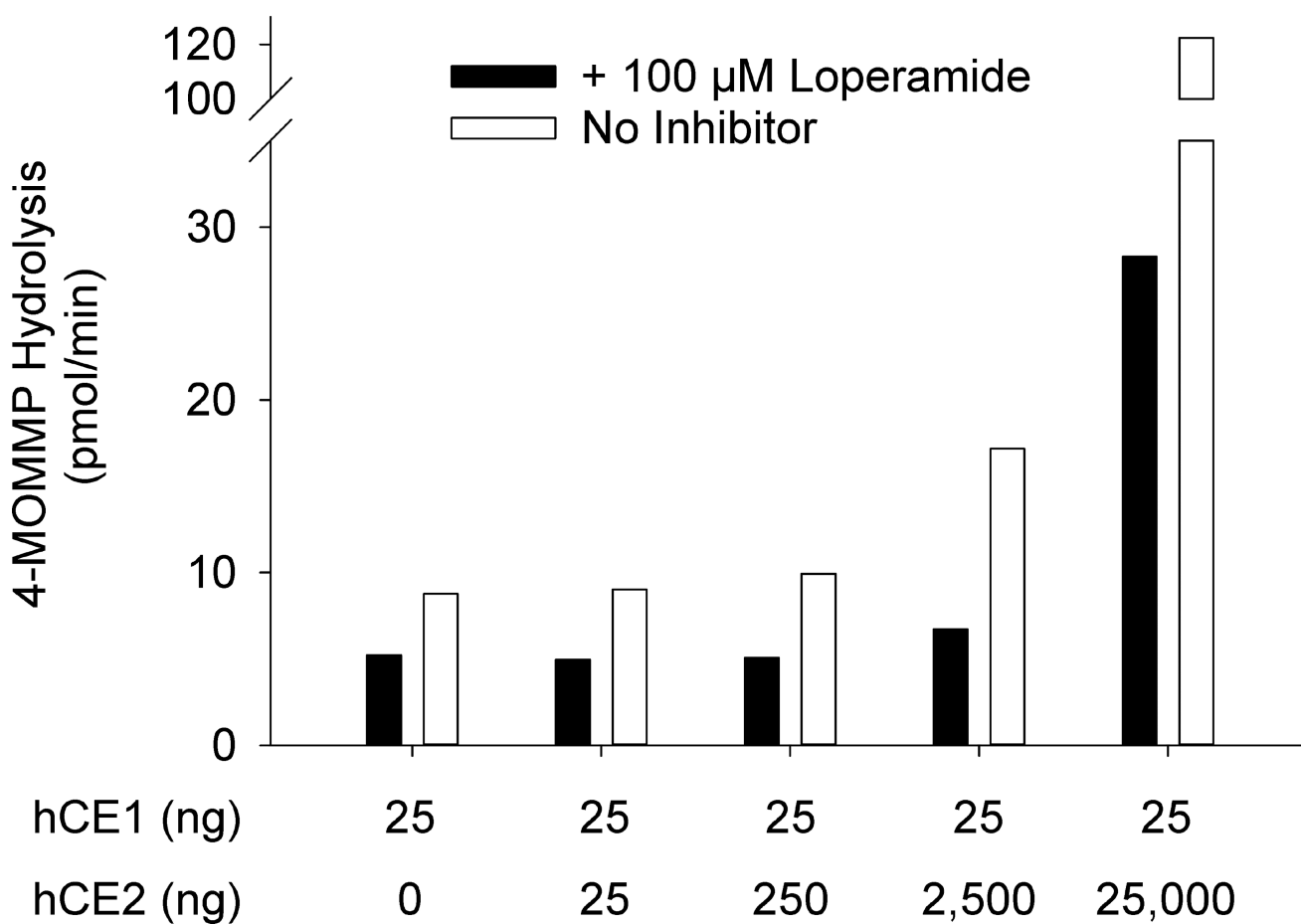
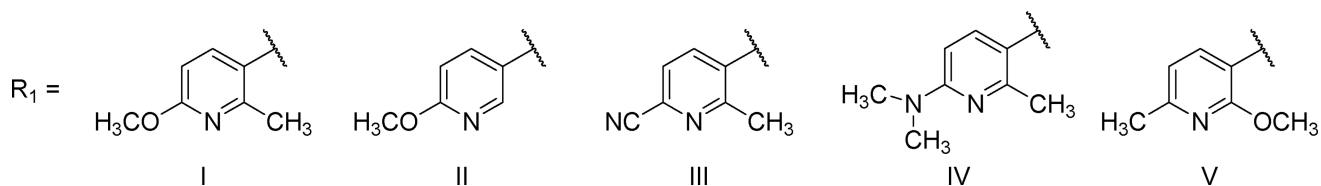
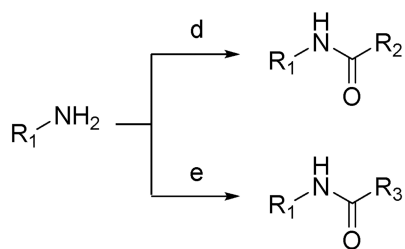
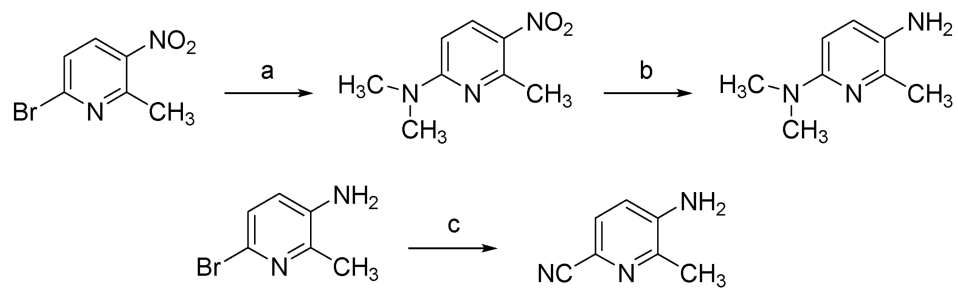


Figure 3.

Effect of loperamide, a selective hCE2 inhibitor, on the selectivity of 4-MOMMP for hCE1. Hydrolysis of 4-MOMMP (50 μ M) was measured with hCE1 (25 ng) and varying concentrations of hCE2 (25–25000 ng). Values represent the average of triplicates for a single experiment.

**Synthetic Scheme.**

a) dimethylformamide, 160°C, *b)* Pd/C, H₂, MeOH, *c)* NaCN, KI, CuI, N,N'-Dimethylethylenediamine *d)* R₂-COCl, methylmorpholine, CH₂Cl₂, 0°C to rt, *e)* R₃-COOH, dimethylaminopyridine, 1-ethyl-3-(3-dimethylaminopropyl)carbodiimide, CH₂Cl₂

Table 1

Maximum λ_{exc} and λ_{em} and relative fluorescence intensity of each fluorophore. Fluorescence was measured at 37°C in phosphate buffer (100 mM, pH = 8, 0.1 mg/mL BSA) containing 1% DMSO.

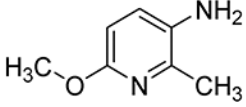
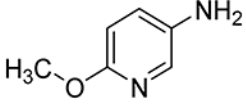
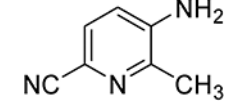
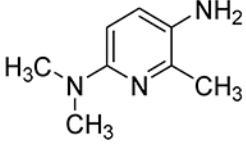
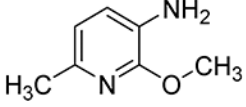
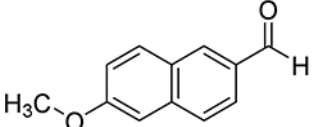
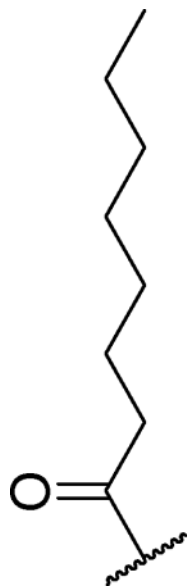
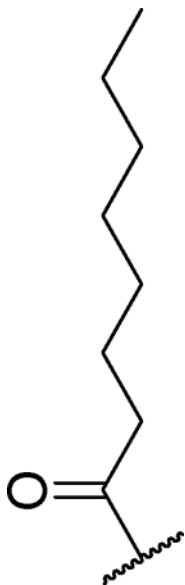
No.		Maximum λ_{exc} (nm)	Maximum λ_{em} (nm)	Relative Fluorescence Intensity (RFU/nmol)
I		304	394	4,400
II		304	398	3,100
III		276	380	3,100
IV		328	432	3,400
V		292	364	1,100
VI		320	462	2,600

Table 2

Specific activity of hCE1, hCE2, hCE3, and FAAH towards octanamides with varying fluorescent cores. Substrate activities ($[S] = 50 \mu\text{M}$) were measured at 37°C in phosphate buffer (100 mM, pH = 8, 0.1 mg/mL BSA) containing 1% DMSO. Values represent the average of triplicates for a single experiment.



No.	R	hCE1 ^a	hCE2 ^b	hCE3 ^c	FAAH ^d
		Specific activity ($\text{pmol}\cdot\text{min}^{-1}\cdot\mu\text{g}^{-1}$)			
CMNA		3000	11000	150	13
1a		440	33	6.0	66
1b		24	21	6.6	480
1c		63	4.4	<1	12



No.	R	hCE1 ^a	hCE2 ^b	hCE3 ^c	FAAH ^d
		Specific activity (pmol.min ⁻¹ .μg ⁻¹)			
1d		54	42	<1	210
1e		1,300	110	2.8	130
1f		950	1,200	3.5	640

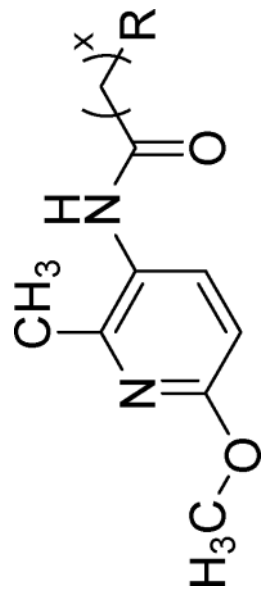
^aValues were calculated based on estimated 25% purity.

^bValues were calculated based on estimated 4% purity.

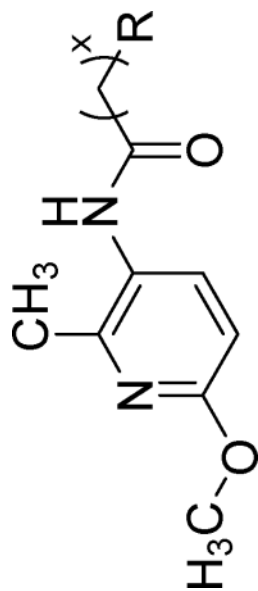
^cValues were calculated based on estimated 3% purity.

^dValues were calculated based on estimated 6.9% purity.

Specific activity of hCE1, hCE2, hCE3, and FAAH towards 2-methyl-6-methoxy-3-pyridinyl amides with varying acyl chains. Substrate activities ([S] = 50 μ M) were measured at 37°C in phosphate buffer (100 mM, pH = 8, 0.1 mg/mL BSA) containing 1% DMSO. Values represent the average of triplicates for a single experiment.

Table 3

No.	R	x	hCE1 ^a	hCE2 ^b	hCE3 ^c	Ratio	
			<1	<1	<1	hCE1/hCE2	hCE1/hCE3
Specific activity (pmol.min ⁻¹ . μ g ⁻¹)							
2		0	1.1	<1	<1	<1	n/a
3		2	6.8	14	<1	<1	0.5
4		4	53	36	2.3	<1	1.5
5		5	180	28	3.9	<1	6.4
1a		6	440	33	6.0	<1	13
6		7	390	37	8.5	<1	11
7		8	130	30	10	<1	4.3
8		10	19	29	9.8	<1	0.7
9		12	2.6	25	7.8	<1	0.1
10		0	<1	<1	<1	<1	n/a
11		1	<1	<1	<1	<1	n/a



No.	R	x	hCE1 ^a	hCE2 ^b	hCE3 ^c	Ratio
			hCE1/hCE2	hCE2/hCE3	hCE3/hCE2	hCE1/hCE2
Specific activity (pmol.min ⁻¹ .μg ⁻¹)						
12		0	2.3	3.2	<1	0.7
13		1	2.9	<1	<1	n/a
14		2	6.3	7.1	<1	0.9
15		3	190	4.9	<1	38.8
16		4	93	18	<1	5.2
17		5	52	5.4	1.6	9.6
18		7	82	30	10	2.7
19 (4-MOMMP)		0	450	13	<1	35
20		0	510	18	4	28

^aValues were calculated based on estimated of 25%.

^bValues were calculated based on estimated of 4%.

^cValues were calculated based on estimated of 3%.

Table 4

Kinetic properties of **1a**, **19**, **20** and CMNA on hCE1 and hCE2. Values for V_{\max} and K_M were determined by non-linear regression of activities from 6 different substrate concentrations (100 μM , 50 μM , 25 μM , 12.5 μM , 6.25 μM and 3.13 μM) at 37°C in phosphate buffer (100 mM, pH = 8, 0.1 mg/mL BSA) containing 1% DMSO. Values represent the average of triplicates for a single experiment.

	1a	4-MOMMP	20	CMNA
hCE1				
V_{\max}^{app} ($\text{pmol}\cdot\text{min}^{-1}\cdot\mu\text{g}^{-1}$)	380	480	680	1,400
K_M (μM)	25	28	15	5
$V_{\max}^{\text{app}}/K_M$ ($\text{pmol}\cdot\text{min}^{-1}\cdot\mu\text{g}^{-1}\cdot\mu\text{M}^{-1}$)	15	17	45	280
hCE2				
V_{\max}^{app} ($\text{pmol}\cdot\text{min}^{-1}\cdot\mu\text{g}^{-1}$)	14	4	31	9,600
K_M (μM)	18	8.9	30	8.3
$V_{\max}^{\text{app}}/K_M$ ($\text{pmol}\cdot\text{min}^{-1}\cdot\mu\text{g}^{-1}\cdot\mu\text{M}^{-1}$)	0.78	0.45	1.0	1,200

Table 5

Limit of detection (LOD) and limit of quantification (LOQ) for hCE1 using partially purified enzyme. Substrate activities ($[S] = 50 \mu\text{M}$) were measured at 37°C in sodium phosphate buffer (100 mM, pH = 8, 0.1 mg/mL BSA) containing 1% DMSO. The signal-to-noise ratio was determined by taking the ratio of the mean signal to the standard deviation of the background signal, each performed as quadruplicates of a single experiment.

	Kinetic Mode ^a	Endpoint mode		
		1 hour	4 hours	24 hours
4-MOMMP				
LOD ^b	3.9 ng	0.06 ng	0.03 ng	0.008 ng
LOQ ^c	16 ng	2.0 ng	0.12 ng	0.03 ng
CMNA				
LOD ^b	2.0 ng	0.98 ng	3.9 ng	0.06 ng
LOQ ^c	3.9 ng	7.8 ng	(-) ^d	(-) ^d

^aKinetic measurements were taken at 30 second intervals for 30 minutes.

^bLOD is the lowest measurement where $S/N > 3$.

^cLOQ is the lowest measurement where $S/N > 9$.

^dThe (-) indicates that there were insufficient data points above $S/N > 9$ to generate a linear curve.

Specific activity of various tissue lysates for 4-MOMMP and CMNA. Values represent the average of triplicates for a single experiment or the average \pm standard deviation of 3 independent experiments (run in triplicate).

Table 6

	4-MOMMP Hydrolysis		CMNA Hydrolysis		Estimated % of hCE1 in Tissue from Western Blotting ^a
	Specific Activity (pmol/min/ μ g)	Estimated % hCE1 in Tissue from activity	Specific Activity (pmol/min/ μ g)	Estimated % hCE1 in Tissue from activity	
hCE1	370 \pm 27	-	3,000	-	-
hCE2	6.4 \pm 0.7	-	11,000	-	-
hCE3	1.4 \pm 0.4	-	150	-	-
Intestine	<0.05	<0.01%	74 \pm 3	2.5%	0.04%
Kidney	<0.05	<0.01%	15 \pm 5	0.50%	<0.02%
Liver	5.5 \pm 0.4	1.5%	180 \pm 30	6.0%	3%
Lung	0.20 \pm 0.02	0.05%	13 \pm 1	0.43%	0.09%

^aThe concentrations of hCE1, hCE2, and hCE3 in the tissue lysates were estimated by Western blot analyses.

Table 7

Potency of various inhibitors for carboxylesterases and selected serine hydrolases. Inhibitor potencies (IC_{50}) were measured at 37°C in phosphate buffer (100 mM, pH = 8, 0.1 mg/mL BSA) containing 2% DMSO using either CMNA (hCE1, hCE2, hCE3, AADAC, PON1) or **1b** (FAAH) as the substrate ($[S]_{final} = 50 \mu\text{M}$). Values represent the average of triplicates for a single experiment.

	IC_{50} (μM)		
	2-chloro-3',4'-dimethoxybenzil	Loperamide	Thyroxine
hCE1	2.5	>100	1.5
hCE2	0.014	0.65	16
hCE3	>100	>100	23
AADAC	>100	23	0.73
FAAH	7.6	>100	>100
PON1	25	>100	2.1
Selectivity hCE2/hCE1	180	>150	0.094